DOI: 10.1002/asia.200700135

Germanates of 1D Chains, 2D Layers, and 3D Frameworks Built from Ge–O Clusters by Using Metal-Complex Templates: Host–Guest Symmetry and Chirality Transfer

Guang-Zhen Liu,[a] Hong-Xia Zhang,[a] Zhi-En Lin,[a] Shou-Tian Zheng,[a] Jie Zhang,[a] Jing-Tai Zhao,[b] Guo-Ming Wang,[c] and Guo-Yu Yang*[a]

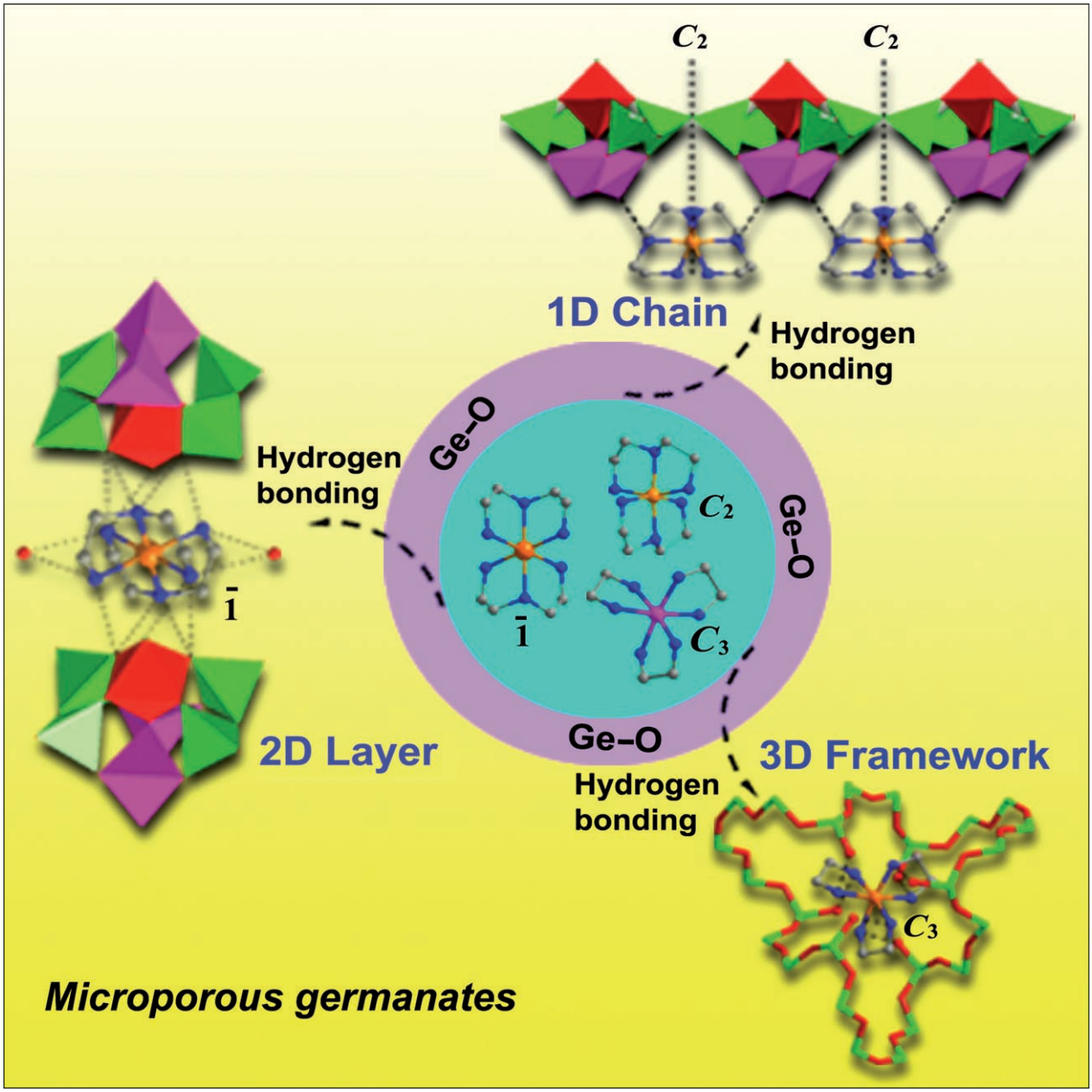

Abstract: The self-assembly of Ge–O polyhedra by metal-complex templates leads to initial examples of open germanate structures under mild solvothermal conditions. These materials are constructed from Ge–O cluster building bocks (Ge_7X_{19} (X = O, OH, or F) or $Ni@Ge_{14}O_{24}(OH)_3$) and span the full range of dimensionalities from 1D chains of $Ge_7O_{13}(OH)_2F_3{\cdot}Cl{\cdot}2[Ni(dien)_2]$ (FJ-**6**) to 2D layers of $Ge_7O_{14}F_3{\cdot}0.5[In(dien)_2]{\cdot}0.5H_3dien{\cdot}2H_2O$ (**1**) and 3D frameworks of $Ni@Ge_{14}O_{24}(OH)_3{\cdot}2[Ni(L)_3]$ (FJ-**1a**/FJ-**1b**) (dien = diethylenetriamine, L = ethylenediamine (en) or 1,2-diaminopropane (enMe)). The Ge_7X_{19} cluster in FJ-**6** and **1** is formed by condensation of four GeX_4 tetrahedra, two GeX_5 trigonal bipyramids, and one GeX_6 octahedron with a μ_3-O atom at the center of the cluster, whereas the $Ni@Ge_{14}O_{24}(OH)_3$ cluster in FJ-**1a**/FJ-**1b** is formed by condensation of nine peripheral GeO_4 tetrahedra and five interior GeO_3Ni units with one μ_5-Ni atom at the center of the cluster. FJ-**6** is characterized by a pair of racemic $Ge_7O_{14}(OH)_2F_3$ cluster chains and represents only one example of 1D germanates; **1** exhibits unique germanate layers with uniform 10-membered-ring apertures encapsulating an unknown indium complex, and the framework structure of FJ-**1a**/FJ-**1b** with large 24-membered-ring channels is the first example of porous materials that contain metal–metal bonds (Ge^{2+}–Ni^{+}). These initial examples of germanates from metal-complex templates provide a useful model system for understanding the mechanisms of host–guest interactions, which may further facilitate the design and development of new porous materials "on demand". It is shown that the symmetry and configuration of the guest metal complex can be imprinted onto the host inorganic framework through hydrogen bonding between host and guest.

Keywords: chirality transfer · germanium · metal complexes · microporous materials · template synthesis

Introduction

The advent of new crystalline porous oxides is of continued interest in solid-state chemistry because of their great impact in catalysis, separation, and ion exchange.[1–3] This class of solids was initially composed of aluminosilicate zeolites constructed from corner-sharing metal–oxygen tetrahedra. However, the discovery of microporous $AlPO_4$ by Flanigen and co-workers[4] in the early 1980s spurred widespread enthusiasm in the synthesis of non-aluminosilicate-based microporous materials with unknown framework topologies, novel framework polyhedral geometries and connectivities, and "record-breaking" pore sizes, such as the microporous compounds VPI-5 (18-membered ring; 18-MR),[5] VSB-1 (24-MR),[6a] ND-1 (24-MR),[6b] and SU-M (30-MR).[7]

Lately, interest in microporous germanates has been steadily growing[8] after the discovery of the first germanate with an open framework by Xu and co-workers[9] at the beginning of the 1990s. Interest in using germanium as a framework-forming element is not only because it is the element chemically closest to silicon but also because of its flexible coordination behavior (tetrahedron, square pyramid or trigonal bipyramid, and octahedron), significantly greater T–O bond distances (≈1.76 Å for Ge–O and ≈1.61 Å for Si–O), and associated smaller T–O–T angles (120–135° for Ge–O–Ge and 140–145° for Si–O–Si) than those in most silicates.[10] The geometrical parameters make germanates particularly favorable candidates for the formation of frameworks with 3-MR channels in a strain-free manner, which is thought to be the key to very open frameworks.[11] Furthermore, germanium is capable of forming cluster aggregates that offer great opportunities for the design of open frameworks with large channels, as predicted by Férey in terms of scale chemistry and defined as the "cluster-condensation" mechanism.[12] The $Ge_7O_{16}X_3$ (X = OH, F) (Ge_7) and $Ge_9O_{22}X_4$ (Ge_9) secondary building units (SBUs) were noted as robust cluster building units and can be used to build extra-large pore systems as shown in ASU-12[8i] with 3D interconnected eight-, 10-, and 16-ring channels and in

[a] G.-Z. Liu, H.-X. Zhang, Z.-E. Lin, S.-T. Zheng, Prof. Dr. J. Zhang, Prof. Dr. G.-Y. Yang
State Key Laboratory of Structural Chemistry
Fujian Institute of Research on the Structure of Matter
and Graduate School of the Chinese Academy of Sciences
Fuzhou, Fujian 350002 (China)
Fax: (+86) 591-8371-0051
E-mail: ygy@fjirsm.ac.cn

[b] Prof. Dr. J.-T. Zhao
State Key Laboratory of High Performance Ceramics and Superfine Microstructure
Shanghai Institute of Ceramics
Chinese Academy of Sciences
Shanghai 200050 (China)

[c] Dr. G.-M. Wang
Department of Chemistry
Teachers College of Qingdao University
Qingdao, Shandong 266071 (China)

ASU-16[8c] (also SU-12[8e]) with 24-ring channels, whose structures are based on the different arrangements of the Ge_7 clusters. Another example of a 24-ring germanate is FDU-4,[8j] which is built by the connection of corner-sharing $Ge_9O_{18}(OH)_4$ clusters. More recently, Zou and co-workers[8q] demonstrated that the different building units of Ge_7 and Ge_9 clusters can also be combined into the same framework structure, for example, SU-8 and SU-44 with 3D interconnected eight-, 10-, and 16-MR channels and eight-, 10-, 16-, and 18-MR channels, respectively. Notably, they reported in a previous work[7] a crystalline mesoporous germanate (SU-M) with 30-MR extra-large channels (>20 Å), which is built from a unique Ge_{10} cluster and has the lowest framework density of any inorganic material.

Although a complete and detailed understanding of the mechanisms of formation of microporous compounds is currently difficult, several models account for the final framework structures by postulating various building blocks from the viewpoint of host infrastructure, such as the SBU model[13,14] and the chain-self-assembly model.[15] Inasmuch as such solids are usually made by hydrothermal routes in the presence of various templates, in some cases by encapsulating them with a very close fit between the templates and the pore walls, it is necessary to investigate the assembly process of framework polyhedra by the templates from the viewpoint of host–guest interactions.[16–17] It has been shown that host–guest charge and symmetry matching are important synthetic parameters for the self-assembly process of porous materials wherein the shape, size, and charge of guest templates can determine the host framework,[8a,f,18–23] whereas the origin of this phenomenon is less clear. Thus, the selection of proper templates to direct to "particular" framework structures is a useful approach for a better understanding of the origin of the host–guest matching. In contrast to alkali-metal ions and organic amines, rigid metal complexes used as templates, which exhibit various charges, unique spatial configurations, and rich hydrogen-bonding sites, have shown great advantages in the synthesis of novel open-framework materials such as phosphates,[24] phosphites,[25] and borophosphates.[26] Remarkably, it was shown that a chiral metal complex as a guest can imprint its chiral characteristics onto the inorganic host framework of phosphates through the noncovalent interactions between host and guest.[24a–d] Unfortunately, versatile metal complexes as templates are absent from the literature with regard to microporous germanates, except for ICMM-2, which contains an extra-framework linear complex $[M(NH_3)_2]$ ($M=Ag^+$ or Cu^+),[27] and several examples in which the transition-metal (Zn, Co, Cd, In) complexes were incorporated with the framework.[28]

We are focusing on the synthesis of open-framework materials constructed from Ge–O clusters[28d,29] and are dedicated to investigating the effect of the introduction of heteroatoms, such as boron (+3 oxidation state),[30–33] on their framework topologies. As a part of our ongoing research, we are currently interested in extending the unique performance of versatile metal complexes to the germanate system and further understanding its role in determining the host framework structures of germanates. In this work, by structure elucidation of initial examples of germanates constructed from the linkage of cluster units by using metal-complex templates, we attempt to give new insight into the self-assembly process of porous solids from the viewpoint of host–guest interactions. These materials span a range of dimensionalities from the 1D chain of $Ge_7O_{13}(OH)_2F_3{\cdot}Cl{\cdot}2[Ni(dien)_2]$ (FJ-**6**)[34] to the 2D layer of $Ge_7O_{14}F_3{\cdot}0.5[In(dien)_2]{\cdot}0.5H_3dien{\cdot}2H_2O$ (**1**) and the 3D frameworks of $Ni@Ge_{14}O_{24}(OH)_3{\cdot}2[NiL_3]$ (FJ-**1a**/FJ-**1b**)[35] (dien = diethylenetriamine, L = ethylenediamine(en) for FJ-**1a**, 1,2-diaminopropane (enMe) for FJ-**1b**). It is shown that the occurrence of shape-controlled synthesis for such materials by using metal-complex templates coincides with the host–guest symmetry and configuration correspondence that result from the hydrogen-bonding interactions between the framework and template, which also provide a useful model system for a better understanding of the self-assembly of host framework polyhedra by guest templates, and may further facilitate the rational design and development of certain predicted porous materials.

Abstract in Chinese:

溶剂热条件下，过渡金属配合物模板剂导向合成了1D链 $Ge_7O_{13}(OH)_2F_3{\cdot}Cl{\cdot}2[Ni(dien)_2]$ (FJ-**6**), 2D层 $Ge_7O_{14}F_3{\cdot}0.5[In(dien)_2]{\cdot}0.5H_3dien{\cdot}2H_2O$ (**1**), 及3D框架结构 $Ni@Ge_{14}O_{24}(OH)_3{\cdot}2[Ni(L)_3]$ (FJ-**1a**/FJ-**1b**) (dien = diethylenetriamine, L = ethylenediamine (en)/1,2-diaminopropane (enMe))。FJ-**6**是目前仅有的一例1D锗酸盐，结构中金属配合物的手性特征传递到 $\{Ge_7O_{14}(OH)_2F_3\}_n$ 簇链；**1**的锗酸盐层含有10-MR结构，层间填充着铟配合物；FJ-**1a**/FJ-**1b**具有24-MR超大孔道，它是首例含有金属-金属键的孔材料，同时发现：金属配合物客体的手性及对称性通过主—客体间的氢键作用传递到无机主体骨架。

Results and Discussion

Synthesis

The germanates in question were synthesized by using solvothermal technology. FJ-**6** and **1** were prepared with pyridine as solvent in the presence of HF. Notably, the existence of HF in the synthetic process was necessary for the formation of the two compounds. FJ-**6** was initially obtained from a mixture containing H_3BO_3 designed for the synthesis of a borogermanate;[34] H_3BO_3 was later removed from the reaction system, and it was found that the synthesis could still be carried out. Furthermore, powder X-ray diffraction showed that a phase-pure sample with FJ-**6** framework topology could also be obtained as polycrystallites by using $[Co(dien)_2]^{2+}$ as template cations. For **1**, the unknown $[In(dien)_2]^{3+}$ complex cations are self-organized in the reaction medium and play the role of a cooperative template with the organic amine in the formation of the inorganic networks. When In_2O_3 was removed from the reaction system,

CHEMISTRY
AN ASIAN JOURNAL

a new layered germanate, $Ge_7O_{14}F_3(H_2dien)_{1.5}\cdot H_2O$,[36] with the ASU-20[8l] framework structure was isolated. FJ-**1a**/FJ-**1b** was initially obtained by using ethylene glycol as solvent in the presence of $[NiL_3]Cl_2\cdot 2H_2O$ (L = en, enMe) as template.[35] The synthesis conditions of FJ-**1a**/FJ-**1b** were not very critical: a phase-pure sample with high crystallinity was isolated either by using pyridine instead of ethylene glycol as solvent or by the replacement of $[NiL_3]Cl_2\cdot 2H_2O$ with a mixture of $NiCl_2\cdot 2H_2O$ and en or enMe in the original reaction system. However, when other transition metals and amines, such as Mn^{2+}, Fe^{2+}, Cu^{2+}, Zn^{2+}, or Cd^{2+} and en were used instead of Ni^{2+}or In^{3+} and enMe or dien, no structures similar to **1**, FJ-**1**, or FJ-**6** were formed. Crystallographic and refinement details for **1** are summarized in Table 1. The morphology of **1** is shown in Figure 1.

Table 1. Crystal data and structure-refinement parameters for **1**.

Parameters	**1**
Empirical formula	$C_6N_{4.5}H_{25}Ge_7In_{0.5}O_{16}F_3$
M_r [g mol^{-1}]	1038.84
Crystal system	monoclinic
Space group	*C*2/*c*
a [Å]	35.875(4)
b [Å]	14.1723(14)
c [Å]	10.4110(9)
a [°]	90
β [°]	101.832(4)
γ [°]	90
V [Å^3]	5180.8(9)
Z	8
ρ_{calcd} [g cm^{-3}]	2.664
λ [Å]	0.71073 ($Mo_{K\alpha}$)
μ [mm^{-1}]	8.543
Reflections collected	19658
Independent reflections	5924 (R(int) = 0.0703)
Refined parameters	323
GOF on F^2	1.107
$R1$, $wR2$ ($I > 2\sigma(I)$)	0.0622, 0.1265
Largest diff. peak, hole [e Å^{-3}]	1.327, −0.971

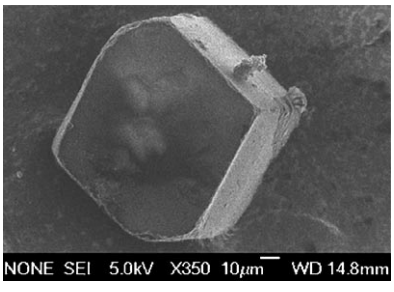

Figure 1. Scanning electron microscopy image of **1**.

Crystal Structures of the 1D and 2D Phases

The structures of FJ-**6**[34] and **1** are constructed from a Ge_7X_{19} (X = O, OH, or F) cluster unit (Figure 2), in which seven Ge atoms exhibit mixed coordination of four to six with O or F anions. The center of gravity of the cluster nearly coincides with a tricoordinated oxygen atom, which is

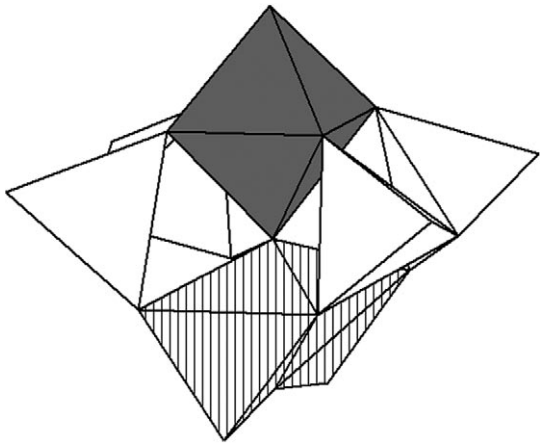

Figure 2. Polyhedral view of the Ge_7X_{19} (X = O, OH, or F) cluster unit of FJ-**6** and **1**. Tetrahedra are shown in white, trigonal bipyramids are striped, and the octahedron is in gray.

bound to an octahedral and two trigonal-bipyramidal Ge centers. Two pairs of corner-sharing tetrahedral Ge atoms are linked to the octahedral and trigonal-bipyramidal Ge sites by doubly bridging oxygen atoms in their equatorial planes. Whereas all the Ge polyhedra are connected to each other by their vertices, the two trigonal bipyramids are linked by a common edge. The Ge_7X_{19} cluster unit can also be described as a D4R unit, which is present in zeolites, AlPOs,[37–40] and some germanates,[8c,29,41,42] with two neighboring tetrahedral atoms replaced by one capping octahedral Ge atom. The location of the central tricoordinated oxygen atom within the cluster unit is similar to that of a fluorine or an oxygen atom that is typically observed within the D4R cage.

Similar Ge_7X_{19} cluster units were observed in ASU-12,[8i] ASU-16,[8c] ASU-19,[8l] ASU-20,[8l] and $Ge_{10}O_{21}(OH)\cdot N_4C_6H_{21}$[8k] by using different bases as templates. Seven of the anions in this cluster are singly coordinated and available for linkage when the clusters condense into a framework, but the presence of partly terminal anions can prevent the Ge_7X_{19} clusters from completely connecting, thus generating interrupted structures. For example, in ASU-12[8i] and ASU-16,[8c] the clusters are linked by the sharing of five vertices into five-connected nets that result from prismatic stacking of planar 6^3 and 4.8^2 nets, respectively. Furthermore, the layers of ASU-20[8l] are four-connected 4^4 nets, which are further connected in pairs by additional isolated GeO_4 linkages to produce the slab structure of ASU-19.[8l] However, in $Ge_{10}O_{21}(OH)\cdot N_4C_6H_{21}$,[8k] the Ge_7X_{19} clusters are linked to each other by additional isolated GeO_4 tetrahedra to produce a 3D framework with a relatively dense noninterrupted structure in which no terminal anion is present.

The structure of FJ-**6** consists of 1D anionic chains of $Ge_7O_{14}(OH)_2F_3$ clusters linked by μ_2-O1 atoms from two tetrahedral Ge centers (Figure 3a). Of the five singly coordinated anions in each cluster, two on the remaining tetrahedral Ge centers are hydroxy groups and three related to the

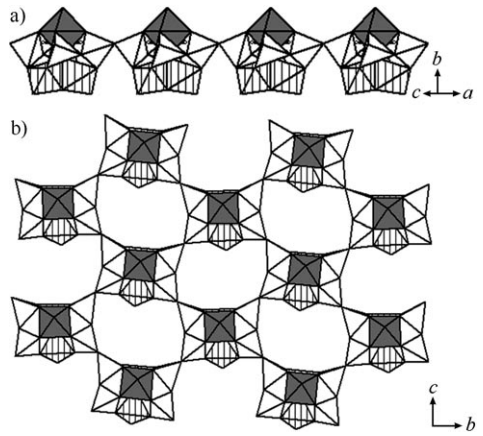

Figure 3. a) The inorganic chain running along the *a* direction in FJ-**6**. b) The inorganic sheet parallel to the *bc* plane in **1**. Tetrahedra are shown in white, trigonal bipyramids are striped, and octahedra are in gray.

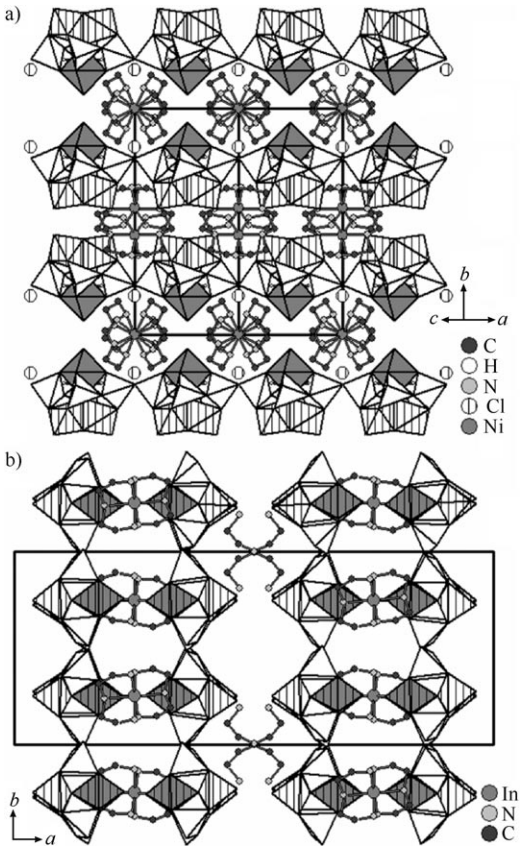

Figure 4. a) Polyhedral view along the [101] direction of FJ-**6** showing the packing of the metal complexes between the inorganic chains. b) Polyhedral view along the [001] direction of **1** showing the alternate array of the indium complex and the H_2dien cations between the inorganic layers. Guest water molecules are omitted for clarity. Tetrahedra are shown in white, trigonal bipyramids are striped, and octahedra are in gray.

octahedral and two trigonal-bipyramidal Ge centers are fluorine atoms. In the 2D phase **1**, each $Ge_7O_{16}F_3$ cluster unit is connected to four adjacent clusters by sharing μ_2-O5 and -O12 atoms of tetrahedral Ge centers to give rise to the same layer topology as ASU-20[8l] (four-connected 4^4 square lattice; Figure 3b). The singly coordinated anions associated with the octahedral and two trigonal-bipyramidal Ge centers are terminal fluorine atoms. However, the sheets in **1** contain uniform 10-MR apertures instead of the alternate eight- and 12-MR openings in ASU-20,[8l] which is attributed to the highly flexible intercluster Ge–O–Ge bond angles and different cluster orientations in the inorganic layers. The Ge–O–Ge bond angles between the clusters are in the range 142.8(4)–151.3(4)° for **1** and 131.9(3)–141.8(5)° for ASU-20,[8l] whereas the intracluster Ge–O–Ge angles remain confined around an average value of 119° (≈118.9° for **1** and 119.1° for ASU-20[8l]) that is independent of the framework structure. Similar values were also found for ASU-12[8i] and ASU-16.[8c]

The geometrical parameters for FJ-**6** and **1** remain within a range typical for germanates. In **1**, the Ge–O bond length for the tetrahedral Ge atoms is between 1.713(6) and 1.769(6) Å, and the O–Ge–O angle is in the range 104.7(3)–115.9(3)°. The Ge–O bond length for trigonal-bipyramidally coordinated atoms varies from 1.773(6) to 2.051(5) Å, and the average Ge–F bond length is 1.814(5) Å. The octahedrally coordinated Ge atom has an expected longer Ge–X distance in the range 1.811(5)–2.016(5) Å.

Hexacoordinated dien complexes of transition metals have been known for a long time[43] and usually have *s-fac*, *u-fac*, and *mer* configurations; the latter two are chiral. In FJ-**6**, there exist two unique Ni sites that correspond to the two isomers *s-fac*-$[Ni1(dien)_2]^{2+}$ and *mer*-$[Ni2(dien)_2]^{2+}$, respectively; no *u-fac*-$[Ni1(dien)_2]^{2+}$ isomer is incorporated. The alternate arrangement of $[Ni(dien)_2]^{2+}$ and the inorganic chain gives rise to a 3D super-molecule network (Figure 4a). In the [100] projection, each inorganic chain is surrounded by five $[Ni(dien)_2]^{2+}$ stacks that interact with the chains electrostatically and through hydrogen bonds, with N···O and N···F distances of 2.888(6)–3.299(7) and 3.023(6)–3.153(7) Å, respectively. There is also hydrogen bonding between isolated Cl^- anions and the N atoms of $[Ni(dien)_2]^{2+}$, with N···Cl distances in the range 3.396(6)–3.589(6) Å.

However, in **1**, the crystallographically distinct In^{3+} cation, which exists in an octahedral environment of two chelating dien ligands, has an *s-fac* configuration; no *u-fac*-$[In(dien)_2]^{3+}$ and *mer*-$[In(dien)_2]^{3+}$ isomers are incorporated. The indium complex $[In(dien)_2]^{3+}$ has not been reported until now. In–N bond lengths are between 2.244(8) and 2.261(8) Å and are comparable with those of transition-metal complexes;[43] the N–In–N angle varies between 79.2(3) and 180.0(1)°. The Ge–O inorganic layers in **1** are stacked in an ABCD sequence along the [100] direction, with the indium complexes and triprotonated dien molecules inserted alternately in the interlamellar space (Figure 4b). The 10-MR channels within the two adjacent layers that encapsulate the indium complexes are relatively well-aligned, whereas the adjacent layers that encapsulate the triprotonated dien molecules are staggered: a 10-MR channel in one

layer faces a $Ge_7O_{16}F_3$ cluster unit in the next layer. Such a layered arrangement generates a 1D system of zigzagged pseudo-10-MR channels along the [100] direction with indium complexes located within the channels. In fact, the indium complexes and the triprotonated dien molecules are located at the unit-cell inversion center, which results in two possible orientations of the dien molecules due to the statistical disorder of the N5 and C6 atoms. Close examination of the guests reveals that the amine groups of the complex cations and the dien molecules interact with the lattice oxygen atom, the terminal fluorine atom in the framework, and the water guests through extensive hydrogen bonding, with N···O and N···F distances in the range 2.800(2)–3.293(10) and 2.765(15)–3.125(9) Å, respectively.

Crystal Structure of the 3D Phase

FJ-**1a** and FJ-**1b** are composed of two isostructural frameworks[35] built by a novel $Ni@Ge_{14}O_{24}(OH)_3$ cluster unit (Figure 5a). The $Ni@Ge_{14}O_{24}(OH)_3$ cluster is composed of one Ni center, 14 Ge centers, 24 O centers, and three OH units. The Ni^+ ion is located at the center of the $Ni@Ge_{14}O_{24}(OH)_3$ unit and is bound to five Ge^{2+} ions by Ge^{2+}–Ni^+ bonds to yield a trigonal-bipyramidal core {$Ni@Ge_5$} (three Ge4 atoms in the equatorial plane and two Ge3 atoms at apical positions). Nine peripheral tetrahedral Ge^{IV} sites (six Ge1 and three Ge2 atoms) form three trimers (Ge_3O_{10}) through corner sharing, and each trimer is further linked to four Ge^{II} centers of the cluster core by μ_2-O atoms. However, each Ge2 center connects a terminal oxygen atom that belongs to hydroxide ligands.

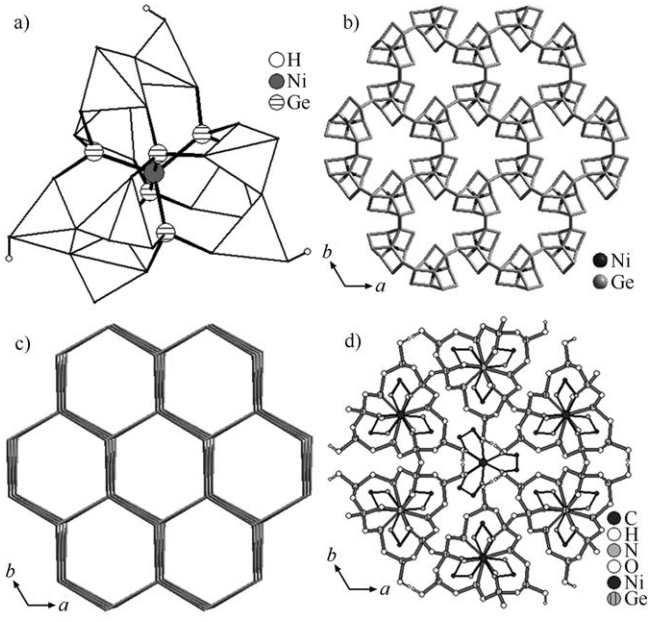

Figure 5. a) Polyhedral and ball-and-stick view of the $Ni@Ge_{14}O_{24}(OH)_3$ cluster unit of FJ-**1a** built from 14 germanium sites and a central nickel site. GeO_4 tetrahedra are shown in white. b) Topological framework of FJ-**1a** showing the 24-ring channels and the $Ni@Ge_{14}O_{24}(OH)_3$ motifs. c) The six-connected nodes are reticulated into a decorated version of the six-connected **acs** net (Schläfli symbol $4^9.6^6$), a hexagonal ABA array. d) View of the orderly separation of the chiral $[Ni2(en)_3]^{2+}$ complexes at the center of the 24-ring channel and the achiral trigonal-prismatic $[Ni3(en)_3]^{2+}$ complexes occluded between the $Ni@Ge_{14}O_{24}(OH)_3$ clusters along the [001] direction.

Each $Ni@Ge_{14}O_{24}(OH)_3$ cluster is linked to six other clusters by Ge–O2–Ge bonds to form a 3D framework (Figure 5b) that contains large 24-MR channels along the [001] direction, which intersect with three 12-ring channels along the [100], [010], and [110] directions. The overall network is a decorated version of the **acs** net (Schläfli symbol $4^9.6^6$),[44,45] which has a rarely observed underlying topology (a hexagonal ABA array) in which each six-coordinate vertex is replaced by an $Ni@Ge_{14}O_{24}(OH)_3$ cluster unit (Figure 5c). Interestingly, two types of $[Ni(en)_3]^{2+}$ complexes are encapsulated in the channels of FJ-**1a** (Figure 5d): one is a regular octahedral $[Ni2(en)_3]^{2+}$ cation, the other is a rare trigonal-prismatic $[Ni3(en)_3]^{2+}$ cation that resulted from the statistical disorder of N2 atoms chelating en ligands. The enantiomers of the $[Ni2(en)_3]^{2+}$ complexes located in the centers of the 24-MR channels are alternately arranged as Λ and Δ configurations along the [001] direction, whereas the $[Ni3(en)_3]^{2+}$ cations that reside in the 12-ring channels are separated by $Ni@Ge_{14}O_{24}(OH)_3$ motifs along the [001] direction. There is extensive hydrogen bonding between the N atoms of the two types of complexes and the framework O atoms, with N···O distances in the range 3.072(16)–3.167(20) Å. Notably, the existence of Ni^+ and Ge^{2+} is considered to be an important factor for the blue luminescence of FJ-**1**.[35]

Framework–Template Interactions

An understanding of framework–template interactions and the role of the template in microporosity generation is of importance not only for new insight into the mechanisms of formation of the microporous frameworks; it could also lead to a rational design of such materials. Upon examining the symmetries of the host framework and guest template on the basis of the structures described here, we surprisingly found that the condensation of framework polyhedra around template molecules is dictated by the molecular symmetries of the latter.

In FJ-**6**, each unit cell contains a pair of racemic anionic cluster chains denoted the left- and right-handed configurations (Figure 6a). Notably, each left-/right-handed chain has the same C_2 symmetry as the chiral $[Ni2(dien)_2]^{2+}$ cations and is related to the chiral $[Ni2(dien)_2]^{2+}$ cation stack by sharing twofold axes in such a way that the metal complex with the Λ configuration is associated with the left-handed chain, and the metal complex with the Δ configuration is associated with the right-handed chain. In other words, there exists a symmetry and configuration correspondence between the chiral complexes and the inorganic chains. A detailed examination of hydrogen bonding reveals that each chiral $[Ni2(dien)_2]^{2+}$ cation forms two hydrogen bonds with the corresponding chiral inorganic chain (Figure 6b), and

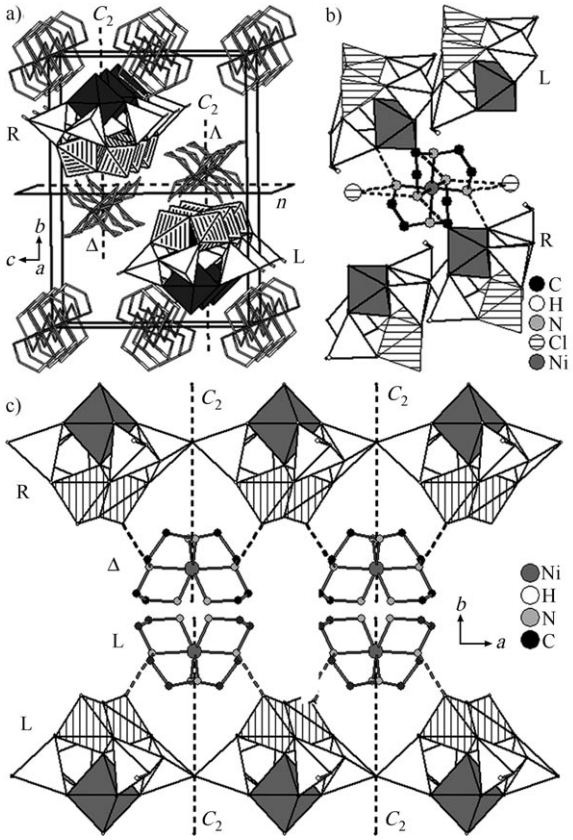

Figure 6. Representations of the host–guest symmetry and configuration correspondence in FJ-**6**. a) Stacking of the racemic anionic cluster chains and metal complexes in one unit cell viewed along the *a* axis. b) Hydrogen bonding between the racemic anionic cluster chains and corresponding chiral complex templates viewed along the *c* axis. c) View of the centrosymmetric H-bonding between the achiral $[Ni1(dien)_2]^{2+}$ complex and the racemic anionic cluster chains as well as two guest Cl^- anions. Tetrahedra are shown in white, trigonal bipyramids are striped, and octahedra are in gray. L and R refer to the left and right chiral chain, respectively.

that these hydrogen bonds are also related by a twofold symmetry axis. This implies that hydrogen bonding imposes a C_2 symmetry operation of the chiral complex templates onto the inorganic chains, thus imbibing them with chiral characteristics in the assembly process of the Ge–O polyhedra. There exists a pair of enantiomers of *mer*-$[Ni2(dien)_2]^{2+}$ related by an *n* glide plane in FJ-**6**, which leads to the chirality and racemization of the inorganic chains. Furthermore, an achiral complex with the *s-fac*-$[Ni1(dien)_2]^{2+}$ configuration also exists; it is located at the unit-cell inversion center, which produces a central symmetry microenvironment related to a pair of adjacent racemic chains and two chlorine anions through hydrogen bonding (Figure 6c). The combination of central and plane symmetry operations leads to the achiral crystal structure of FJ-**6**.

In contrast to FJ-**6**, only *s-fac*-$[In(dien)_2]^{3+}$ complex cations with $\bar{1}$ symmetry are encapsulated between the inorganic layers in **1**. The stacking fashion of the inorganic layers is completely determined by the *s-fac*-$[In(dien)_2]^{3+}$ cations, all of which are located at an inversion center that coincides with the $\bar{1}$ symmetry element of each individual *s-fac*-$[In(dien)_2]^{3+}$ cation. In other words, the condensation of the inorganic layers around the guest metal complexes is dictated by the symmetry of the latter. At the same time, the hydrogen bonds between the indium complex cation and two cluster units from adjacent layers as well as two guest water molecules are related by an inversion center (Figure 7). It

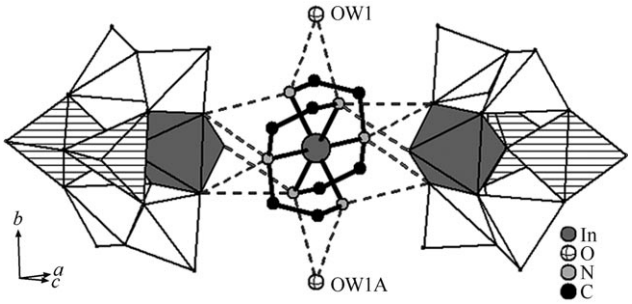

Figure 7. View of the centrosymmetric H-bonding between the achiral $[In(dien)_2]^{3+}$ complex and two cluster units from adjacent layers as well as two interlayer water molecules in **1**. Tetrahedra are shown in white, trigonal bipyramids are striped, and octahedra are in gray.

was shown that a rigid metal complex exerts its symmetry-templating effect through hydrogen bonding.[46–48] By comparison, the flexible dien cation has a relatively weak templating effect and adjusts its molecular conformation with a disordered model to conform to the higher symmetry of the inorganic framework.

The assembly of the inorganic framework of FJ-**1**[35] by metal complexes can be understood as a shape-controlled process. Its 3D framework structure is characteristic of a pair of enantiomers of a propellane-like chiral structural motif denoted the Δ and Λ configurations (Figure 8a and b, respectively). The significance of giving prominence to a structure with such chiral inorganic motifs becomes apparent once it is recognized that the propellane-like structural motif and the chiral complex cation ($[Ni2(en)_3]^{2+}$) both have the same D_3 symmetry, and that each chiral structural motif is assembled by a chiral metal-complex cation ($[Ni2(en)_3]^{2+}$) in such a way that the metal complex with the Δ configuration is closely related to the chiral motif with the Λ configuration and vice versa (Figure 8a and b). This remarkable stereospecific correspondence between the metal-complex template and the structure of the inorganic host clearly indicates that there exists molecular recognition between the guest and the host, which allows the configuration and symmetry information of the guest template to be imprinted onto the inorganic framework through hydrogen-bonding interactions. The alternate stacking of the pair of enantiomers of $[Ni2(en)_3]^{2+}$ along the [001] direction related by a mirror plane (Figure 8c) leads to the chirality and isomerization of the propellane-like structural motif and produces the achirality of the overall structure of FJ-**1a**, with the achiral $[Ni3(en)_3]^{2+}$ cation situated on the plane exhibiting a trigonal-prismatic configuration. Similarly, only sym-

CHEMISTRY
AN ASIAN JOURNAL

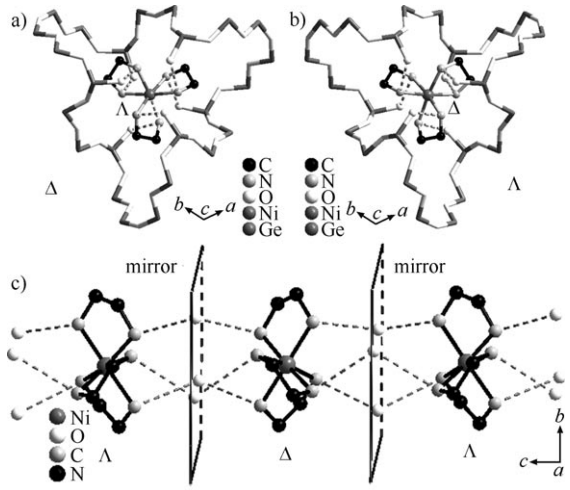

Figure 8. Representations of the host–guest symmetry/configuration correspondence in FJ-**1a**, showing the hydrogen bonds between a pair of enantiomers of the propellane-like chiral motif with a) Δ and b) Λ configuration and the corresponding enantiomers of chiral Λ- and Δ-$[Ni2(en)_3]^{2+}$ complexes. c) A pair of enantiomers of chiral Λ- and Δ-$[Ni2(en)_3]^{2+}$ complexes that alternately reside in the 24-MR channels interacts with six O6H groups from the chiral structure motifs through six hydrogen bonds.

metry correspondence between the achiral $[Ni3(en)_3]^{2+}$ complex and the building bocks of the $Ni@Ge_{14}O_{24}(OH)_3$ cluster exists in FJ-**1**.

The preceding discussion shows that the remarkable correspondence between the symmetry/configuration of the metal-complex template and the structure of the inorganic host is a general feature for the materials described herein, and hydrogen bonding between the host and guest allows the information of the guest template to be imprinted onto the inorganic framework. In situ Raman spectroscopy showed[23] that the template configuration is considered to be intimately related to the framework-forming species and determines the final structure of the porous aluminophosphate material. Moreover, it was expected that a mixed-configuration template could favor the formation of different microporous structures. Interestingly, only the *s-fac*-$[In(dien)_2]^{3+}$ isomer was incorporated into the structure of **1**, and an orderly separation of chiral and achiral complexes in FJ-**1** and FJ-**6** was also found. This indicates the molecular-recognition capability and stereospecificity of the host framework for guest template configuration, which is more than the general understanding that the equilibrium distribution of the various isomeric forms of a metal complex as depending considerably on environmental parameters such as ion association, solvation, temperature, intramolecular nonbonding interactions, and statistical weighting factors.[49] Nevertheless, as discussed above, the use of an achiral metal complex or a pair of racemic isomers of a metal complex as a template is prone to the introduction of additional central or plane symmetry elements in the solids. Given that a crystal structure formed from enantiomerically pure chiral molecules is always chiral,[50,51] it is conceivable that the synthesis of a chiral or even an optically pure porous solid may be realized by using an enantiomerically pure metal-complex template and/or a judicious choice of framework-forming species to influence the template configuration.

Thermal Analysis

Compared with FJ-**6** and FJ-**1a**, which is stable up to 350 and 300 °C, respectively, **1** is stable up to about 200 °C. Subsequently, decomposition occurs in three steps with a total weight loss of 21.8 %. An initial gradual weight loss of 3.7 % between 200 and 250 °C corresponds to the loss of two interlayer guest water molecules per formula unit (calcd: 3.5 %). The latter two steps cover a wide temperature range of 240–920 °C and is accompanied by a weight loss of 18.1 %, which corresponds to the departure of organic amines and 1.5 HF molecules per formula unit (calcd: 17.8 %). The relatively high thermal stabilities of the materials are due to the extensive hydrogen-bonding and electrostatic interactions between the inorganic frameworks and metal-complex templates.

Conclusions

Mild solvothermal methods resulted in initial examples of novel open germanate materials by using metal complexes as templates, whose structures are constructed from the direct linkage of cluster units and range from 1D chains to 2D layers and 3D frameworks. The successful syntheses of such materials suggest further opportunities for isolating new microporous germanates formed from metal-complex templates in a systematic way. The structure elucidation reveals that there is a good correspondence of symmetry and configuration between the guest metal complex and the host inorganic framework. The origin of this phenomenon is attributed to hydrogen bonding between host and guest. It is highly likely that the host–guest symmetry and configuration correspondence leads to the shape-controlled synthesis for such materials in the presence of metal-complex templates and plays a more general role in the formation of many other microporous materials. Therefore, this study provides new insight into their mechanisms of formation. Given that such host–guest correspondence can determine the characteristics of the inorganic framework, and that an achiral or a pair of racemic isomers of the metal-complex template is prone to the introduction of additional central or plane symmetry elements in the solids, the synthesis of a chiral or even optically pure crystalline porous germanate material may ultimately be realized by using an enantiomerically pure metal-complex template and/or a judicious choice of framework-forming species to influence the template configuration. Investigations in this direction are underway.

Experimental Section

Materials and Instrumentation

All syntheses were performed in a 23-mL teflon-lined stainless-steel autoclave under autogenous pressure. Reagents were obtained from commercial sources and used without further purification. Elemental analysis of C, H, and N was performed on an Elemental Vario EL III analyzer. Infrared (IR) spectra were obtained from powder samples as KBr pellets on an ABB Bomen MB 102 series IR spectrophotometer over a frequency range of 400–4000 cm^{-1}. Qualitative energy-dispersive spectroscopy (EDS) was performed on a JEOL JSM6700F field-emission scanning electron microscope equipped with an Oxford INCA system. Thermogravimetric analysis (TGA) was performed on a Mettler Toledo TGA/SDTA 851e analyzer under N_2 atmosphere with a heating rate of 10 °C min^{-1}.

Syntheses

1: Typically, germanium dioxide (0.152 g, 1.46 mmol) and indium dioxide (0.141 g, 0.51 mmol) were dispersed in a mixed solvent of pyridine (4.5 mL) and water (1 mL), and then dien (2.5 mL) followed by HF (40 wt%, 0.15 mL) was added with constant stirring. The resulting mixture was sealed in a 23-mL teflon-lined autoclave, heated at 180 °C for 7 days, and then cooled to room temperature. The product containing a white polycrystalline powder and colorless prism-shaped single crystals was separated by sonication, further washed by distilled water, and then air-dried (45.2% yield based on GeO_2). IR (KBr): $\tilde{\nu}$ = 3450, 3256, 1603, 1539, 1458, 1347, 1146, 1082, 992, 878, 798, 592, 533, 474, 414 cm^{-1}; elemental analysis: calcd (%) for $C_{12}N_9H_{50}Ge_{14}InO_{32}F_6$: C 6.94, H 2.41, N 6.06; found: C 6.98, H 2.51, N 6.12; EDS: Ge/In/F calcd: 7:0.5:3; found: 6.8:0.5:2.7.

X-ray Crystallography

Suitable single crystals with dimensions 0.10 × 0.10 × 0.02 mm^3 for **1** were selected for single-crystal X-ray diffraction analysis. Data were collected on a Siemens SMART CCD diffractometer with graphite-monochromated $Mo_{K\alpha}$ radiation (λ = 0.71073 Å) at 293 K. All absorption corrections were performed with the SADABS program.[52] The structure was solved by direct methods and refined by full-matrix least-squares methods on F^2 with the SHELXTL97 program package.[53] The N5 and C6 atoms of the dien molecule were refined with a model of splintering due to the special position of the molecule, and soft constraints were also applied on the C–C and C–N bond lengths of the disordered dien molecule; the C1 atom of the $[In(dien)_2]^{3+}$ cation was also disordered over two sites. All hydrogen atoms, except those on the disordered C and N atoms and guest water molecules, were positioned geometrically and refined with a riding model. All non-hydrogen atoms except those disordered atoms were refined anisotropically. The position of the highest peak (1.327 e $Å^{-3}$) in the final Fourier map was near that of the disordered dien molecule. In **1**, the inorganic Ge–O layers are connected to two different templates, H_3dien and $[In(dien)_2]$, through hydrogen-bonding interactions to form an open-framework structure, which gave rise to voids of 216 A^3. Such voids in the crystal structure are common in microporous materials. For example, the 24-MR-channel zinc phosphate ND-1[6b] contains voids of 285 A^3, which resulted from the exceptionally porous structure.

CCDC-205575, -628446, -277021, and -280327 (FJ-**6**, **1**, FJ-**1a**, and FJ-**1b**, respectively) contain the supplementary crystallographic data for this paper. These data can be obtained free of charge from the Cambridge Crystallographic Data Centre at www.ccdc.cam.ac.uk/data_request/cif.

Acknowledgements

This work was supported by the 973 Program (No. 2006CB932900), the NNSF of China (Nos. 20473093 and 20271050), the NSF of Fujian Province (Nos. E0510030 and 2004J043), and the Key Program of the CAS (No. KJCX2-YW-H01).

[1] *Introduction to Zeolite Science and Practice: Studies in Surface Science and Catalysis* (Eds.: H. van Bekkum, E. M. Flanigen, P. A. Jacobs, J. C. Jansen), Elsevier, New York, **2001**.
[2] A. K. Cheetham, G. Férey, T. Loiseau, *Angew. Chem.* **1999**, *111*, 3466; *Angew. Chem. Int. Ed.* **1999**, *38*, 3268.
[3] M. E. Davis, *Nature* **2002**, *417*, 813.
[4] S. T. Wilson, B. M. Lok, C. A. Messina, T. R. Cannan, E. M. Flanigen, *J. Am. Chem. Soc.* **1982**, *104*, 1146.
[5] M. E. Davis, C. Saldarriaga, C. Montes, J. M. Graces, C. Crowder, *Nature* **1988**, *331*, 698.
[6] a) N. Guillou, Q. Gao, M. Nogues, R. E. Morris, M. Hervieu, G. Férey, A. K. Cheetham, *Acad. Sci. Paris Ser. II* **1999**, *2*, 387; b) G.-Y. Yang, S. C. Sevov, *J. Am. Chem. Soc.* **1999**, *121*, 8389.
[7] X. Zou, T. Conradsson, M. Klingstedt, M. S. Dadachov, M. O'Keeffe, *Nature* **2005**, *437*, 716.
[8] a) X. Bu, P. Feng, G. D. Stucky, *J. Am. Chem. Soc.* **1998**, *120*, 11204; b) H. Li, O. M. Yaghi, *J. Am. Chem. Soc.* **1998**, *120*, 10569; c) H. Li, M. Eddaoudi, D. A. Richardson, O. M. Yaghi, *J. Am. Chem. Soc.* **1998**, *120*, 8567; d) C. Cascales, E. Gutiérrez-Puebla, M. A. Monge, C. Ruíz-Valero, *Angew. Chem.* **1998**, *110*, 135; *Angew. Chem. Int. Ed.* **1998**, *37*, 129; e) H. Li, M. Eddaoudi, O. M. Yaghi, *Angew. Chem.* **1999**, *111*, 682; *Angew. Chem. Int. Ed.* **1999**, *38*, 653; f) X. Bu, P. Feng, G. D. Stucky, *Chem. Mater.* **1999**, *11*, 3025; g) T. Conradsson, X. Zou, M. S. Dadachov, *Inorg. Chem.* **2000**, *39*, 1716; h) C. Cascales, E. Gutiérrez-Puebla, M. Iglesias, M. A. Monge, C. Ruíz-Valero, N. Snejko, *Chem. Commun.* **2000**, 2145; i) J. Plévert, T. M. Gentz, A. Laine, H. Li, V. G. Young, O. M. Yaghi, M. O'Keeffe, *J. Am. Chem. Soc.* **2001**, *123*, 12706; j) Y. Zhou, H. Zhu, Z. Chen, M. Chen, Y. Xu, H. Zhang, D. Zhao, *Angew. Chem.* **2001**, *113*, 2224; *Angew. Chem. Int. Ed.* **2001**, *40*, 2166; k) L. Beitone, T. Loiseau, G. Férey, *Inorg. Chem.* **2002**, *41*, 3962; l) J. Plévert, T. M. Gentz, T. L. Groy, M. O'Keeffe, O. M. Yaghi, *Chem. Mater.* **2003**, *15*, 714; m) M. E. Medina, M. Iglesias, N. Snejko, E. Gutiérrez-Puebla, M. A. Monge, *Chem. Mater.* **2004**, *16*, 594; n) M. E. Medina, E. Gutiérrez-Puebla, M. A. Monge, N. Snejko, *Chem. Commun.* **2004**, 2868; o) L. Tang, M. S. Dadachov, X. Zou, *Chem. Mater.* **2005**, *17*, 2530; p) N. Snejko, M. E. Medina, E. Gutiérrez-Puebla, M. A. Monge, *Inorg. Chem.* **2006**, *45*, 1591; q) K. E. Christensen, L. Shi, T. Conradsson, T. Ren, M. S. Dadachov, X. Zou, *J. Am. Chem. Soc.* **2006**, *128*, 14238.
[9] a) J. Cheng, R. Xu, *J. Chem. Soc. Chem. Commun.* **1991**, 483; b) J. Cheng, R. Xu, G. Yang, *J. Chem. Soc. Dalton Trans.* **1991**, 1537; c) R. H. Jones, J. Chen, J. M. Thomas, A. George, M. B. Hursthouse, R. Xu, S. Li, Y. Lu, G. Yang, *Chem. Mater.* **1992**, *4*, 808; d) S. Li, R. Xu, Y. Lu, Y. Xu in *Proceedings of the 9th International Zeolite Conference* (Eds.: R. von Ballmoos, J. B. Higgins, M. M. J. Treacy), Butterworth-Heinemann, Boston, **1992**, p. 345.
[10] M. O'Keeffe, O. M. Yaghi, *Chem. Eur. J.* **1999**, *5*, 2796.
[11] P. O. Brunner, W. M. Meier, *Nature* **1989**, *337*, 146.
[12] G. Férey, *J. Solid State Chem.* **2000**, *152*, 37.
[13] R. Szostak, *Molecular Sieves: Principles of Synthesis and Identification*, Van Nostrand Reinhold, Toronto, **1989**.
[14] G. Férey, *J. Fluorine Chem.* **1995**, *72*, 187.
[15] a) J. W. Richardson, Jr., J. V. Smith, J. J. Pluth, *J. Phys. Chem.* **1990**, *94*, 3365; b) E. B. Keller, W. M. Meier, R. M. Kirchner, *Solid State Ionics* **1990**, *43*, 93; c) H. Li, M. E. Davis, J. B. Higgins, R. M. Dessau, *J. Chem. Soc. Chem. Commun.* **1993**, 403; d) S. Oliver, A. Kuperman, G. A. Ozin, *Angew. Chem.* **1998**, *110*, 48; *Angew. Chem. Int. Ed.* **1998**, *37*, 46.
[16] a) S. L. Burkett, M. E. Davis, *J. Phys. Chem.* **1994**, *98*, 4647; b) P. K. Dutta, M. Puri, *J. Phys. Chem.* **1987**, *91*, 4329; c) D. Grandjean, A. M. Beale, A. V. Petukhov, B. M. Weckhuysen, *J. Am. Chem. Soc.* **2005**, *127*, 14454.
[17] a) W. C. Paik, C. H. Shin, J. M. Lee, B. J. Ahn, S. B. Hong, *J. Phys. Chem. B* **2001**, *105*, 9994; b) B. Han, S. H. Lee, C. H. Shin, P. A. Cox, S. B. Hong, *Chem. Mater.* **2005**, *17*, 477; c) L. Gomez-Hortiguela, F. Cora, C. R. A. Catlow, J. Perez-Pariente, *J. Am. Chem. Soc.* **2004**, *126*, 12097.
[18] P. Feng, X. Bu, G. D. Stucky, *Nature* **1997**, *388*, 735.
[19] X. Bu, P. Feng, G. D. Stucky, *Science* **1997**, *278*, 2080.

[20] P. Feng, X. Bu, S. H. Tolbert, G. D. Stucky, *J. Am. Chem. Soc.* **1997**, *119*, 2497.
[21] X. Bu, P. Feng, T. E. Gier, D. Zhao, G. D. Stucky, *J. Am. Chem. Soc.* **1998**, *120*, 13389.
[22] X. Bu, P. Feng, G. D. Stucky, *Chem. Mater.* **2000**, *12*, 1505.
[23] M. G. O'Brien, A. M. Beale, C. R. A. Catlow, B. M. Weckhuysen, *J. Am. Chem. Soc.* **2006**, *128*, 11745.
[24] a) K. Morgan, G. Gainsford, N. Milestone, *J. Chem. Soc. Chem. Commun.* **1995**, 425; b) J. Yu, Y. Wang, Z. Shi, R. Xu, *Chem. Mater.* **2001**, *13*, 2972; c) Y. Wang, J. Yu, Y. Li, Z. Shi, R. Xu, *Chem. Eur. J.* **2003**, *9*, 5048, and references therein; d) Y. Wang, J. Yu, M. Guo, R. Xu, *Angew. Chem.* **2003**, *115*, 4223; *Angew. Chem. Int. Ed.* **2003**, *42*, 4089; e) D. A. Bruce, A. P. Wilkinson, *J. Chem. Soc. Chem. Commun.* **1995**, 2059; f) D. A. Bruce, A. P. Wilkinson, M. G. White, J. A. Bertand, *J. Solid State Chem.* **1996**, *125*, 228; g) M. J. Grey, J. D. Jasper, A. P. Wilkinson, *Chem. Mater.* **1997**, *9*, 976; h) K. R. Morgan, G. J. Gainsford, N. B. Milestone, *Chem. Commun.* **1997**, 61; i) S. M. Stalder, A. P. Wilkinson, *Chem. Mater.* **1997**, *9*, 2168; j) J. D. Jasper, A. P. Wilkinson, *Chem. Mater.* **1998**, *10*, 1664; k) D. J. Williams, J. S. Kruger, A. F. McLeroy, A. P. Wilkinson, J. C. Hanson, *Chem. Mater.* **1999**, *11*, 2241; l) Y. Wang, P. Chen, J. Li, J. Yu, J. Xu, Q. Pan, R. Xu, *Inorg. Chem.* **2006**, *45*, 4764.
[25] a) Z.-E. Lin, J. Zhang, S.-T. Zheng, G.-Y. Yang, *Eur. J. Inorg. Chem.* **2004**, 953; b) J. Liang, J. Li, J. Yu, P. Chen, L. Li, R. Xu, *J. Solid State Chem.* ***2006***, *179*, 1977.
[26] G.-Y. Yang, S. C. Sevov, *Inorg. Chem.* **2001**, *40*, 2214.
[27] C. Cascales, E. Gutiérrez-Puebla, M. Iglesias, M. A. Monge, C. Ruíz-Valero, *Angew. Chem.* **1999**, *111*, 2592; *Angew. Chem. Int. Ed.* **1999**, *38*, 2436.
[28] a) X. H. Bu, P. Y. Feng, G. D. Stucky, *Chem. Mater.* **2000**, *12*, 1811; b) N. N. Julius, A. Choudhury, C. N. R. Rao, *J. Solid State Chem.* **2003**, *170*, 124; c) D. Pitzschke, W. Bensch, *Angew. Chem.* **2003**, *115*, 4525; *Angew. Chem. Int. Ed.* **2003**, *42*, 4389; d) Z. E. Lin, J. Zhang, S. T. Zheng, G. Y. Yang, *Microporous Mesoporous Mater.* **2004**, *74*, 205.
[29] Z.-E. Lin, S.-T. Zheng, G.-Y. Yang, *Z. Anorg. Allg. Chem.* **2006**, *632*, 354.
[30] Z.-E. Lin, J. Zhang, G.-Y. Yang, *Inorg. Chem.* **2003**, *42*, 1797.
[31] H.-X. Zhang, J. Zhang, S.-T. Zheng, G.-M. Wang, G.-Y. Yang, *Inorg. Chem.* **2004**, *43*, 6148.
[32] G.-M. Wang, Y.-Q. Sun, G.-Y. Yang, *Cryst. Growth Des.* **2005**, *5*, 313.
[33] H.-X. Zhang, J. Zhang, S.-T. Zheng, G.-Y. Yang, *Inorg. Chem.* **2005**, *44*, 1166.
[34] H.-X. Zhang, J. Zhang, S.-T. Zheng, G.-Y. Yang, *Inorg. Chem.* **2003**, *42*, 6595.
[35] Z.-E. Lin, J. Zhang, J.-T. Zhao, S.-T. Zheng, C.-Y. Pan, G.-M. Wang, G.-Y. Yang, *Angew. Chem.* **2005**, *117*, 7041; *Angew. Chem. Int. Ed.* **2005**, *44*, 6881.
[36] Crystallographic data for $Ge_7O_{14}F_3(H_2dien)_{1.5}\cdot H_2O$: space group $C2/c$, $a=16.1027(6)$, $b=16.4573(6)$, $c=17.8138(6)$ Å, $\beta=98.142(2)°$, $V=4673.2(3)$ Å^3, $Z=4$.
[37] M. Estermann, L. B. McCusker, C. Baerlocher, A. Merrouche, H. Kessler, *Nature* **1991**, *352*, 320.
[38] P. Reinert, B. Marler, J. Patarin, *Chem. Commun.* **1998**, 1769.
[39] T. Loiseau, G. Férey, *J. Solid State Chem.* **1994**, *111*, 403.
[40] F. Taulelle, A. Samoson, T. Loiseau, G. Férey, *J. Phys. Chem. B* **1998**, *102*, 8588.
[41] T. Conradsson, M. S. Dadachov, X. Zou, *Microporous Mesoporous Mater.* **2000**, *41*, 183.
[42] M. E. Medina, M. Iglesias, M. A. Monge, E. Gutiérrez-Puebla, *Chem. Commun.* **2001**, 2548.
[43] a) F. G. Mann, *J. Chem. Soc.* **1934**, 466; b) A. Zalkin, D. H. Templeton, T. Ueki, *Inorg. Chem.* **1973**, *12*, 1641; c) A. Zalkin, D. H. Templeton, T. Ueki, *Inorg. Chem.* **1973**, *12*, 1641.
[44] O. Delgado Friedrichs, M. O'Keeffe, O. M. Yaghi, *Acta Crystallogr. Sect. A* **2003**, *59*, 22.
[45] A. C. Sudik, A. P. Côté, O. M. Yaghi, *Inorg. Chem.* **2005**, *44*, 2998.
[46] P. Feng, X. Bu, G. D. Stucky, *Angew. Chem.* **1995**, *107*, 1911; *Angew. Chem. Int. Ed. Engl.* **1995**, *34*, 1745.
[47] X. Bu, P. Feng, G. D. Stucky, *J. Chem. Soc. Chem. Commun.* **1995**, 1337.
[48] X. Bu, P. Feng, G. D. Stucky, *Chem. Mater.* **2000**, *12*, 1505.
[49] E. J. Corey, J. C. Bailar, *J. Am. Chem. Soc.* **1959**, *81*, 2620.
[50] J. Jacques, A. Collet, S. H. Wilen, *Enantiomers, Racemates, and Resolutions*, John Wiley & Sons, New York, **1981**; J. Jacques, A. Collet, Reissue with Corrections, Krieger, Malabar, **1994**.
[51] H. D. Flack, *Helv. Chim. Acta* **2003**, *86*, 905.
[52] G. M. Sheldrick, Program for the Siemens Area Detector Absorption Correction, University of Göttingen, Göttingen (Germany), **1997**.
[53] G. M. Sheldrick, SHELXS-97, Program for the Solution of Crystal Structures, University of Göttingen, Göttingen (Germany), **1997**.

Received: April 19, 2007
Revised: June 8, 2007
Published online: September 4, 2007

